NASA TECHNICAL NOTE

NASA TN D-4966

NASA TN D-4966

MEASUREMENTS OF SOME PROPERTIES OF A DISCHARGE FROM A HOLLOW CATHODE

by George A. Csiky

Lewis Research Center

Cleveland, Ohio

NATIONAL AERONAUTICS AND SPACE ADMINISTRATION • WASHINGTON, D. C. • FEBRUARY 1969

MEASUREMENTS OF SOME PROPERTIES OF A DISCHARGE FROM A HOLLOW CATHODE

By George A. Csiky

Lewis Research Center
Cleveland, Ohio

NATIONAL AERONAUTICS AND SPACE ADMINISTRATION

For sale by the Clearinghouse for Federal Scientific and Technical Information
Springfield, Virginia 22151 – CFSTI price $3.00

ABSTRACT

A mercury-vapor-fed hollow cathode of the type used in SERT II Kaufman thrusters was operated in a bell jar. Voltage-current characteristics and ranges of mercury flow rate and anode distance were determined for the principal observed discharge modes of "spot" and "plume" with discharge currents ranging up to 3 amperes. Plasma potential, electron density, and electron temperature in the uniform potential external discharge were measured by Langmuir probe techniques. Tentative theoretical models of potential distribution are suggested and discussed for the two modes.

CONTENTS

MEASUREMENTS OF SOME PROPERTIES OF A DISCHARGE FROM A HOLLOW CATHODE

by George A. Csiky

Lewis Research Center

SUMMARY

The discharge from a mercury-vapor-fed hollow cathode was studied. The cathode was of the small-orifice (0.015-cm-diam) type used in the SERT II electron bombardment ion thruster both as main cathode and neutralizer. The discharge was operated between the cathode and a planar anode at a few centimeters distance. The system was set up in a bell jar in which the operating pressure was of the order of 10^{-6} torr.

Various modes of operation were observed. The two principal modes were those known as the "spot" and the "plume" mode. A third mode was recognized as a variant of the plume mode with a higher voltage for a given current. Voltage-current discharge characteristics were obtained for each mode, and the approximate limits of the ranges of operating conditions were found. A discharge current range up to 3 amperes was covered.

Langmuir probe measurements showed a nearly equipotential plateau of about 11 volts above the cathode potential extending over the bulk of the discharge region for both principal modes. Values for electron densities and electron temperatures were also obtained from Langmuir probe traces at various positions in the discharge.

Tentative theoretical models were established for the two principal modes. For the spot mode, it appears likely that the near equipotential plateau of the external discharge region penetrates well into the orifice region. When this condition is satisfied, ionization appears to take place mostly inside of, or near, the orifice, and a well-ionized plasma flows out of the cathode.

The plume mode is probably characterized by the edge of the equipotential plateau being at or near the orifice exit plane. Only a few of the electrons accelerated through the cathode sheath will produce ionization before escaping the vicinity of the cathode, so that additional ionization takes place in the luminous plume.

An understanding of the manner in which potential gradients form in a discharge from a hollow cathode will aid in the proper design of the ion chamber geometry and thereby increase thruster efficiency with this type of cathode.

INTRODUCTION

A variety of electrical discharge devices use cathodes in which the discharge originates from a cavity. They are known as hollow cathodes (ref. 1) and they may operate under varied conditions of vapor densities and discharge currents and voltages.

The use of vapor-fed hollow cathodes both as a plasma-bridge neutralizer and as the ion chamber electron source has been advantageous in mercury bombardment ion thrusters (ref. 2). Such hollow cathodes require lower power for operation, have long-expected life, and can be pretested prior to a flight application. The optimum adaptation of a hollow cathode for both applications was intensively investigated in the course of the development of the SERT II experimental thruster (refs. 3 and 4). The demonstrated usefullness of the hollow cathode for the bombardment thruster makes it desirable to understand the detailed physics of its operation as either neutralizer or ion chamber electron source. The experimental measurements and theoretical calculations presented in this report are aimed toward a fundamental physical understanding of hollow-cathode operation in the regimes of interest for thruster applications.

A hollow cathode of the type used in the ion thruster differs from conventional cathodes (e.g., refractory metal ribbon, or oxide magazine) in several important ways. The hollow cathode is a source of mercury atoms, as well as of electrons. A pressure gradient of several orders of magnitude exists just outside the hollow-cathode orifice as mercury vapor expands into a region of low pressure. With the hollow cathode, electron injection into the main discharge region is confined to a much smaller area than with other types of cathodes.

The properties of the external discharge obtained from a hollow cathode also differ from those produced by conventional cathodes. For example, it was necessary to introduce a baffle in the discharge chamber of the electron bombardment thruster to obtain good performance when the discharge was fed by a hollow cathode (ref. 4).

The properties of this external discharge are of interest for improved understanding of both the operation of hollow cathodes as well as their interactions with other electric thruster components. This report presents voltage-current discharge characteristics obtained with an unconfined vacuum discharge operated between a hollow cathode and a planar anode. Discharge currents were investigated over the range from 0.1 milliampere to 3.0 amperes, while cathode-anode spacings from a few millimeters to more than 7 centimeters were used. In addition to the overall voltage-current performance, Langmuir probes were used to determine electron density and temperature within the discharge at an anode-cathode spacing of 3 centimeters. SI units (rationalized mks system) are used throughout this report. All symbols are defined in appendix A.

APPARATUS AND PROCEDURE

Hollow Cathode

A sketch of the longitudinal cross section of the hollow-cathode tip is shown in figure 1. The tip assembly consisted of a 0.32-centimeter outside-diameter tantalum tube with a 0.1-centimeter-thick, 2-percent-thoriated tungsten-alloy disk attached to one end by electron-beam welding. A small orifice was cut in the center of the tungsten disk by a sandblasting process. The sandblasting usually made the exit (downstream) diameter slightly larger than the entrance (upstream) diameter. The measured diameters on the tip used were 0.015 centimeter upstream and 0.025 centimeter downstream. An insert placed inside the tantalum tube facilitated starting the discharge. The insert was made of a 0.001-centimeter-thick tantalum foil coated with a barium carbonate mixture and rolled into a spiral. A cut in the insert formed a cavity of about 0.07 centimeter in diameter and 0.15 centimeter long behind the orifice. The axial channel through the insert was about 0.05 centimeter in diameter. The cathode tube was externally heated electrically by a tungsten-rhenium wire embedded in a flame-sprayed coating of aluminum oxide.

Facility and Experimental Setup

The experiments were conducted in a 45-centimeter-diameter bell jar evacuated by an oil diffusion pump. With a liquid-nitrogen cold trap, the bell jar base pressure was approximately 5×10^{-7} torr, and increased typically to about 1×10^{-6} to 5×10^{-6} torr as mercury flow was added. These were indicated gage readings with no correction made for the presence of mercury. Figure 2 shows the relative location and dimensions of the cathode, anode, keeper electrode, and vaporizer. Figure 3 is a photograph of the cathode apparatus mounted in a bell jar. About 10 wraps of 0.001-centimeter-thick tantalum foil about the cathode served as heat shielding. Except where noted, a ring-like keeper electrode was mounted close to the cathode tip to initiate the discharge and help maintain it electrically stable. The keeper was made of 0.16-centimeter-diameter tantalum wire formed in a loop of 0.6-centimeter inside diameter and was placed in a plane about 0.23 centimeter from the orifice.

The anode was in front of the cathode, directly facing it, at a distance that could be varied. For the runs during which discharge characteristics were studied, a 14-centimeter-diameter circular stainless-steel disk was used as the anode. When the probe data were taken, this anode was replaced by one consisting of annular segments mounted on a boron nitride plate. The segments were 1 centimeter wide with outside diameters of 1, 2.5, 4.0, 5.5, and 7.0 centimeters, respectively. The segmented

anode had been installed for other experiments that are not reported herein. Comparative tests showed that the difference between the solid disk and the segmented anode was not a significant factor in the interpretation of the data in this report.

Mercury was fed to the cathode by a temperature-controlled porous-tungsten vaporizer of the type used to feed the neutralizer in the SERT II thruster (ref. 2). The mercury was supplied from an external precision-bore calibrated glass tube. The average flow rate was determined from periodic readings of the mercury level.

Figure 4 is an electrical circuit schematic of the experimental setup. The discharge power supply was provided with both voltage and current limiting controls. The keeper supply was designed to drop from a high starting voltage to a low operating voltage when the discharge to the electrode started. In the tests where the keeper was not used and the discharge was lit directly to the main anode, the 500-volt supply was used parallel with the anode supply with appropriate switching connections.

Langmuir Probes and Probe Circuit

The discharge was probed with a cylindrical Langmuir probe. The active area of the probe was a 0.3-centimeter-long exposed length of a 0.0076-centimeter-diameter tungsten wire. The probe construction is shown in figure 5. The probe wire extended from the interior of a quartz tube with a thin gap between the wire and the quartz. This gap prevented conduction of current to the probe by any deposit that might possibly form on the insulator. The long axis of the wire was perpendicular to the long axis of the cathode.

Figure 6 shows the probe circuit schematic. A 90-volt battery with a variable resistor was used to bias the probe with respect to the grounded cathode. As the bias voltage was varied, an x-y recorder traced out the probe voltage-current characteristic.

Anode Distance

When the discharge voltage-current characteristics were studied at various anode distances, the keeper electrode was absent and the axial anode position was variable through manual movement of a shaft. The discharge was started directly to the anode that was about 0.2 centimeter from the cathode tip. Once the discharge was lit, it could be maintained over the full range of the anode distance variation, that is, up to 7.2 centimeters.

For taking the probe data, a fixed main anode distance of 3 centimeters was used. The use of the keeper electrode was necessary to start the discharge during these tests.

The position of the probe was axially and laterally variable.

Starting and Transfer of Discharge

For starting the discharge, the cathode tip was heated to about 1100° C. A potential of 300 volts was applied to the keeper (or to the main anode at a near position, when the keeper was absent). Mercury vapor flow was started by heating the vaporizer. The discharge usually started with a flow between 10 and 50 equivalent milliamperes (the current that would exist if each atom carried one electronic charge). Occasionally, higher flow and higher cathode temperatures were required to start the discharge. Transfer of the discharge to the main anode was accomplished simply by applying potential to the main anode. While the keeper was running, it was usually adjusted to draw about 0.1 ampere. The typical corresponding keeper voltage was about 10 volts.

EXPERIMENTAL RESULTS

Observed Modes of Operation: Visual Appearance of Discharge

Early in the experiments, it was observed that at least three distinctly different modes of operation could be obtained depending on the value of the neutral flow, the cathode to anode distance, and the discharge circuit variables. In the highest current mode, the discharge was not visible except for an intense bluish white spot just downstream of the orifice, extending only a few millimeters. This has been referred to as the "spot" mode (ref. 5) and is shown in figure 7(a). The power supply was operated current-limited in the spot mode, with only a low voltage required. A typical value was 2.0 amperes at 13.5 volts.

A generally lower current (or higher voltage) mode was characterized by a visible plume of blue plasma extending forward in a cone several centimeters from the cathode orifice, as shown in figure 7(b). This mode is called the "plume" mode. Sometimes currents comparable to the spot mode could be drawn in the plume mode with voltages of about 40 to 50 volts. More often, however, drawing a high current resulted in sudden transition into the spot mode. Conversely, attempting to operate the spot mode with a low current brought about a drop into the plume mode. The plume mode could be stably operated by limiting the voltage to approximately 35 volts which would result in a current of about 0.3 ampere.

With very low neutral flows and/or large anode distances, a third mode was found. In this mode, only up to 0.3 ampere of discharge current flowed at 60 volts. It had the

appearance of a low-intensity plume mode.

Ranges of Modes

Figure 8 shows the approximate ranges of anode distance and neutral flow in which the various modes were obtained. Low neutral flows and large anode distances tend to lead to the plume mode, while high flows and short distances generally result in the spot mode. A region of overlap is shown between the spot and plume modes. In that overlap region, stable operation of either mode is possible over an appreciable range of discharge currents. At or below 20 milliamperes of neutral flow, it was difficult to maintain anything but a high-voltage plume mode at medium or long anode distances. At very short distances, however, the spot mode was obtained.

Discharge Characteristics

Figure 9 presents a typical voltage-current discharge characteristic for each mode. The spot mode is seen to run at consistently low voltage. The characteristic has a low slope; that is, a large increase in current is obtained for small voltage increments. The plume mode characteristic curve has a minimum. To the right of the minimum, the curve is approximately parallel to that of the spot mode: to the left, there is a rapid rise in voltage with decreasing current. The characteristic curves for the third mode, the high-voltage-plume mode, range up to 0.3 ampere with voltages between 25 and 60 volts. For comparison, one such characteristic is shown in the upper left corner of figure 9.

Langmuir Probe Data

For the Langmuir probe runs, the anode distance was fixed at 3 centimeters. The neutral flow was between 45 and 55 equivalent milliamperes. The bell jar pressure was about 3×10^{-6} torr. Langmuir probe traces were obtained at various probe positions along the symmetry axis of the discharge and at some positions off-axis. The x-y recorder probe traces were transferred to semilogarithmic paper. Typical semilogarithmic plots of traces for the two major modes are shown in figure 10. Appendix B describes briefly how such plots are interpreted to yield values of electron density, plasma potential, and electron temperature. It should be emphasized that while plasma potential and electron temperature can be obtained fairly accurately, values for electron

density, as obtained graphically, may be in error by as much as 40 percent. For the calculations in this report, though, this accuracy is more than sufficient. Comparison of the two curves in figure 10 shows a wider rounding off of the knee in the plume mode than in the spot mode. This is generally indicative of greater fluctuations, or "noise," in the plasma. An oscilloscope check confirmed that the plume mode contained fluctuations of about 1000 cps, while the spot mode was quiet.

In figures 11, 12, and 13 the values of electron density, plasma potential, and electron temperature, as determined from probe traces, are plotted as a function of position. Part (a) of each figure shows the variation of the parameter along the symmetry axis for each mode. Parts (b) are radial plots for the spot mode in a plane normal to the axis and 1 centimeter distant from the cathode tip. Radial plots for the plume mode were not obtained because, for the low electron densities at the off-axis positions, interpretation of the probe traces became uncertain.

DISCUSSION OF RESULTS

A satisfactory theoretical model for the steady-state operation of a hollow cathode is not available at present. Such a model would describe the electron emission mechanism, the flow and spatial density distribution of electrons, ions, and neutrals, the form of the potential gradients, and ion formation in the discharge.

The data obtained in this investigation serve to answer parts of the total problem. The following paragraphs describe tentative models for the spot mode and the plume mode based on the experimental probe data and an estimate of the vapor density inside the hollow cathode and in the region between the cathode and anode. The details of the calculations are given in subsequent sections. The main features of the discharge in the two modes are summarized in table I.

For both modes, the potential in the main body of the discharge has been found to be uniform, typically at about 11 volts above the cathode. It is perhaps significant that, in both modes, the plasma formed at a potential that barely exceeded the first ionization potential of mercury (10.4 V). The boundary of this nearly equipotential plateau where the potential gradient becomes appreciable, will be called the "sheath edge." Further discussion will show that the position where the sheath edge forms near the cathode hole or inside it, appears to be a determining characteristic of the modes. However, in these experiments no probe measurements could be made closer than 0.5 centimeter to the cathode, and thus the position of the sheath edge can only be inferred.

The thickness of the sheath over the cathode surface is of the order of the Debye length,

$$l_D = 7.4\times10^3 \left(\frac{V_e}{n_e}\right)^{1/2} \tag{1}$$

given in mks units, where V_e is the electron temperature, and n_e is the electron number density.

Figure 14 shows two hypothetical sheath-edge positions in the cross sections of a hollow-cathode orifice channel. It is suggested that they are characteristic of the two modes, as indicated.

Spot Mode

The spot mode is characterized by a generally greater plasma density in the discharge region and a lower electrical resistance of the discharge (defined as the discharge voltage divided by the discharge current). A higher rate of mercury flow, shorter cathode-to-anode distance, and a drawing of higher discharge current are factors that tend to produce this mode. Apparently, a stable operation of the spot mode requires a sufficiently high discharge current and a relatively high vapor density both in the tip and in the discharge region.

A high estimate of the Debye length for conditions that may exist inside the hollow cathode in the spot mode (taking $V_e(\max) = 10$ V and $n_e(\min) = 10^{19}$ electrons/m^3) is 7.4×10^{-6} meters, about a thirtieth of the orifice diameter. If a sheath of this thickness is postulated in the hollow-cathode geometry, the equipotential plateau must be assumed to penetrate fully into the hole and the cavity. The exact form of the potential gradient inside the cathode is not known. It is governed by the conditions in the plasma forming in the internal regions. However, it appears evident from calculations given in a later section on the Flow Density of Fast Electrons, that, for the spot mode, it is necessary to assume that the sheath edge forms deep enough in the cathode so that most electrons leaving the sheath are trapped in the orifice region.

The position of the sheath edge postulated for the spot mode enables electrons accelerated through the sheath to ionize before they leave the high-neutral-density region. The electron mean free path for ionization collisions is

$$\lambda_e = \frac{1}{\sqrt{2}\, n \sigma_e} \tag{2}$$

where n is the neutral density, and σ_e is the ionization cross section for mercury.

The cross section for single ionization of neutral mercury atoms by electrons rises rapidly with electron energy above the ionization potential. Its value is about 10^{-20} square meter (ref. 6) for electrons that leave the cathode surface with negligible velocity and gain approximately 11 volts in the sheath. The excitation cross section at this energy is of the same order of magnitude.

Based on an estimated density, $n = 10^{22}$ atoms per cubic meter, the mean free path in the orifice channel is about 10^{-2} meter, which well exceeds the dimension of the orifice diameter (2×10^{-4} m). However, due to reflections from the sheath, fast electrons are trapped in the cavity long enough to produce ionizations there. This mechanism explains - at least quantitatively - the higher electron density (thus higher degree of ionization) observed in this mode. Moreover, since most fast electrons produce ionization or excitation inside or very near the tip, the larger portion of the discharge region between cathode and anode is not luminous. The mean free path for ion-neutral collisions is short enough (of the order of 10^{-4} m) so that many ions are probably carried out the hole assuring that the efflux is essentially a neutral plasma.

Plume Mode

The plume mode has a lower electron number density than the spot mode and presents a higher resistance path to the passage of the discharge current. Apparently, low vapor densities, or the drawing of insufficient discharge current causes the plume mode to prevail. The plasma potential here again is found nearly uniform in most of the region between cathode and anode at about 11 volts with respect to cathode potential. However, the anode potential is much higher (e.g., about 35 V to draw 0.3 A of discharge current).

Tonks and Langmuir (ref. 7) point out that an anode in a discharge will be at plasma potential only if the random electron current impinging on its surface equals the discharge current. If this random current is too low, there is a potential rise at the anode; if it is too large, there is a drop instead. The random current depends on the electron density and the electron temperature in the vicinity of the anode, and also on the anode area.

In the plume mode, the estimated Debye length in the orifice, and hence, the cathode sheath dimension, appears to be of the same order as the orifice dimensions. This leads one to postulate potential gradients such that the sheath edge spans the orifice, as suggested by figure 14(b).

Kemp and Hall (ref. 5) measured floating emissive probe potentials inside and outside a hollow cathode apparently operating in the plume mode. The discharge voltage was 30 volts for a discharge current of 0.13 ampere. They found that the potential was less than 2 volts in the interior of the tip, and it rose sharply to 20 volts within about 0.1 centimeter outside the orifice where a nearly equipotential plateau started which extended almost up to the anode. This measured gradient is compatible with the sheath location indicated in figure 14(b).

The calculation presented in a later section entitled Flow Density of Fast Electrons shows that, with such sheath geometry, only a few of the electrons accelerated through the sheath (which now comprises the entire interior of the tip) will collide with neutrals and ionize them near the cathode. Fast electrons may thus leave the close vicinity of the cathode and cause some ionization and excitation in the region between cathode and anode, which is probably the cause of the luminous appearance of the discharge.

Comparison of Estimated Atom Density and Electron Density

In appendix C, the magnitude of the atom density and its spatial variation in the hollow-cathode efflux is estimated for the absence of a discharge. It is shown there that the estimate is reliable, at least within an order of magnitude, allowing for lack of accurate knowledge of the temperature inside the cathode and also allowing for pressure variation over the length of the orifice channel.

In the presence of a discharge, the atom density is still defined as the density of mercury atoms, including both ionized and neutral. In a region with much backstreaming of ions toward the cathode, the atom density may be appreciably higher than the value estimated for a neutral efflux. However, in the external plasma region where the potential gradients are small, the order-of-magnitude atom-density estimate is probably also valid when a discharge current is drawn. The degree of ionization in the plasma can be inferred by comparing the local atom-density estimates with measured electron densities.

Table II shows these values at various locations for the two modes. The comparison in the table indicates that, in the spot mode, the degree of ionization may be as high as 10 to 100 percent over the entire discharge region, while in the plume mode it is probably at least a decade lower. It should be remembered that both sets of density data involve some uncertainty, thus the inferred degree of ionization can only be regarded as an approximate indication.

Flow Density of Fast Electrons

The sheath edge has been defined as a surface that separates the plasma potential plateau from a region of strong potential gradient known as the "sheath." For concreteness, one may regard the sheath-edge location as an equipotential surface slightly below the plasma potential.

Ionization by electron bombardment occurs when electrons collide with neutral atoms with sufficient kinetic energy to cause the removal of an orbital electron. In a plasma maintained by a discharge, the electrons accelerated through the cathode sheath represent the most important source of energy.

In this section, the estimated atom-density gradient is used to calculate the attenuation of the flow density of fast electrons that leave the sheath edge. It is shown that, under the conditions prevailing in these experiments, a large fraction of the electrons accelerated through the sheath would not be able to ionize within the path length between cathode and anode, if it is assumed that the plane of the sheath edge is essentially normal to the symmetry axis of the discharge. Further considerations have shown that a similar situation prevails even if the sheath edge bulges inward from the exit hole, as long as multiple reflection of the electrons from the walls of the orifice channel is not significant.

For mercury atoms to be singly ionized (ionization potential, 10.4 V) by energy derived from the electrostatic field, electrons must be accelerated over the full width of the sheath to about 11 volts. Therefore, one may regard the sheath edge as a source of fast electrons leaving the surface in the direction of the normal. Let j_e be defined as the particle flux density (electrons/(m^2)(sec)) of fast electrons only. (Symbols and their definitions are also listed in appendix C.) Ionizing and exciting collisions will constitute a sink for this stream and j_e will decrease with distance in the direction of the flow if neutral atoms are present. Elastic scattering may partly randomize this stream, but the scattered intensity predominates for the forward direction. Neglecting this effect and assuming a parallel stream of fast electrons (i.e., one-directional flow) result in the rate of change of the flow density j_e with distance, due to "removals" by ionizing and exciting collisions,

$$\frac{dj_e}{dx} = - j_e(x)n(x)\sigma_e \tag{3}$$

where x is the distance parallel to electron flow.

The neutral density $n(x)$ is a strongly decreasing function of the distance x. It is

shown in appendix C that, in a reasonable approximation, the efflux may be considered to have a cosine distribution; therefore, Knudsen's equation (eq. (B10) of ref. 8) can be used to find the functional form of n(x). For simplicity, conditions along the symmetry axis are considered. On the axis, Knudsen's equation reduces to

$$j(x) = \frac{n_o \bar{v} R^2}{4(x^2 + R^2)} \tag{4}$$

where j(x) is the atom flow density, $\bar{v}$ is the average thermal velocity in the cavity, and R is the radius of the exit hole. At x = 0, the density is taken to be n_o, which may be regarded as a representative value of the density inside the hollow cathode.

The neutral density n(x) at a point P(x) downstream on the symmetry axis is found from the continuity equation

$$n(x) = \frac{2j(x)}{\bar{v}} = \frac{n_o R^2}{2(x^2 + R^2)} \tag{5}$$

since the effective average thermal velocity in the x-direction is $\bar{v}/2$.

Next, equation (5) is substituted into equation (3) and the result integrated from x_s (the position where the sheath edge forms) to some arbitrary point P(x) where the value of $j_e(x)$ is desired (fig. 15 is a representation of the one-dimensional geometry used):

$$\int_{j_e(x_s)}^{j_e} \frac{dj_e}{j_e} = -\sigma_e \int_{x_s}^{x} n\, dx = -\frac{\sigma_e n_o R^2}{2} \int_{x_s}^{x} \frac{dx}{x^2 + R^2} \tag{6}$$

$$\ln \frac{j_e}{j_e(x_s)} = -\frac{\sigma_e n_o R^2}{2} \left(\frac{1}{R} \tan^{-1} \frac{x}{R} \right) \Bigg|_{x_s}^{x} \tag{7}$$

$$j_e(x) = j_e(x_s) \exp \left[\frac{\sigma_e n_o R}{2} \left(\tan^{-1} \frac{x_s}{R} - \tan^{-1} \frac{x}{R} \right) \right] \tag{8}$$

At some large distance from the orifice, that is, where $x >> R$, the value for the fast electron flux density becomes

$$j_e(\infty) = j_e(x_s) \exp\left\{\frac{\sigma_e n_o R}{2}\left[\left(\tan^{-1}\frac{x_s}{R}\right) - \frac{\pi}{2}\right]\right\} \tag{9}$$

This represents a flow of those fast electrons, which fail to produce ionization even over a very long distance, with the form of neutral density distribution assumed. Since $\sigma_e n_o \approx 1/\lambda_{eo}$, where λ_{eo} is the mean free path of the electrons in the cavity, the quantity $1/2\ \sigma_e n_o R$ corresponds approximately to the ratio of the orifice radius to the mean free path of the fast electrons in the interior of the hollow cathode R/λ_{eo}.

In the work described in this report, the value of R/λ_{eo} was at most about 0.01. This makes the exponential of equation (9) very nearly 1 for any value of x_s. This leads to the conclusion that, for the estimated prevailing atom densities, if the sheath edge forms outside the orifice exit hole, only a small portion of the electrons that have been accelerated through the sheath are able to ionize. Most of these electrons reach the anode or the bell jar walls without inelastic collisions.

As mentioned earlier, these conditions appear to correspond to the observed plume mode. Apparently, the relatively few collisions that do occur are capable of maintaining the ion density of the plasma as well as producing the luminous appearance.

For higher values of R/λ_{eo}, the term in parenthesis in equation (9) becomes significant. In figure 16, the ratio $j_e(\infty)/j_e(x_s)$ is plotted against the ratio x_s/R for various values of $1/2\ \sigma_e n_o R$ based on equation (9). Examination of the figure shows that, for higher values of R/λ_{eo} over some range of x_s/R, generally between 1 and 10, there is a transition from a region where most of the fast electrons are captured in ionization ($(x_s/R) \lesssim 1$) to a region where most of them are allowed to escape ($(x_s/R) \gtrsim 10$).

Davis, Walch, and Pinsley (ref. 9) describe the latter region of operation for a different type of hollow cathode as the "electron beam mode," and for that mode they place the lower limit of the ratio of "cathode fall distance to aperture size" at about 10. This observation agrees with the indication of figure 16 if one identifies the mentioned ratio with x_s/R. When x_s/R is about 10 or greater, this identification is certainly valid.

In summary of this derivation, it should be emphasized that the escape of fast electrons is a significant process for only the plume mode. The absence of plume luminosity in the spot mode indicates that most of the emitted electrons have lost considerable energy before entering the plume region. This loss of energy, presumably due to multiple reflections inside the cathode orifice, makes the escape of fast electrons a negligible process in the spot mode.

Emission Mechanism

These results fail to explain the electron emission from the walls of the hollow cathode. For the models assumed, it is necessary that free electrons be available in sufficient number at zero potential at the cathode surface. However, the presence of dissociation or thermal ionization in the plasma will reduce this required number. Also, a small contribution of electrons is to be expected from secondary electrons emitted from the walls on ion impact, even at low energies. It is generally felt that the enhanced emission of hollow cathodes must be explained by a combination of processes.

CONCLUDING REMARKS

A small-orifice, mercury-vapor-fed hollow cathode was operated in a bell jar. Variation of mercury flow, anode distance, or discharge current resulted in various modes of operation. The spot mode was found to be associated with generally higher mercury flow, shorter anode distance, higher discharge current, and lower anode voltage, as compared with the plume mode.

Langmuir probe measurements showed the plasma in the spot mode to be higher in electron density as well as in degree of ionization than it was in the plume mode. Spot mode electron temperatures were about 1.0 to 1.5 volts lower than corresponding values for the plume mode. However, the plasma potential with respect to the cathode was uniform over the bulk of the discharge region between the cathode and the anode and about equal for both modes (about 11 V) in spite of significant differences in anode potentials.

Based on the results of measurements and theoretical calculations, tentative models have been suggested for the spot and plume modes. The spot mode is described as having the equipotential plateau penetrate into the hollow-cathode interior. Electrons have multiple reflections inside the cathode where the neutral density is high, and, therefore, a considerable degree of ionization is obtained.

In the model for the plume mode, a potential gradient exists over most of the inside region of the cathode, and electrons that are accelerated out of the cavity only poorly ionize the neutral efflux, the density of which rapidly drops with distance outside the cathode.

The purpose of this work was to measure fundamental variables and make order-of-magnitude calculations to shed some light on the nature of the operation of the type of

hollow cathode used in ion thrusters. The experimental and theoretical results presented in this report appear to explain some of the observed characteristics of hollow cathodes.

Lewis Research Center,
National Aeronautics and Space Administration,
Cleveland, Ohio, October 2, 1968,
120-26-02-06-22.

APPENDIX A

SYMBOLS

A	area of orifice, m^2
A_{pr}	current collector area of cylindrical Langmuir probe, m^2
e	electronic charge, 1.6×10^{-19} C
J_{Hg}	neutral mercury flow to hollow cathode, atoms/sec
J_I	discharge current, A
J_{pr}	current to probe, A
j	atom flow density, atoms/(sec)(m^2)
j_e	flow density of fast electrons, electrons/(sec)(m^2)
K	Knudsen number
k	Boltzmann constant, 1.38×10^{-23} J/(molecule)(K)
L	length of orifice channel, m
l_D	Debye length, m
m	mass of mercury atom, 3.32×10^{-25}
$\dot{N}$	atom arrival rate, atoms/sec
$\dot{N}_o$	atom arrival rate at upstream end of orifice channel, atoms/sec
n	atom density, atoms/m^3
n_e	electron density, electrons/m^3
n_o	atom density in hollow-cathode cavity, corrected for nonmolecular flow, atoms/m^3
n_o'	atom density in hollow-cathode cavity for molecular flow, atoms/m^3
n_1	atom density in downstream end of orifice
P	arbitrary point labeled by coordinates
R	orifice radius, m
T	temperature, K
V_e	electron temperature, V
ΔV_I	discharge voltage, V

ΔV_{pr} difference in probe bias voltage for one decade of change in current, V

$\bar{v}$ mean molecular velocity, m/sec

x distance from orifice exit hole center along symmetry axis, m

x_s value of x where sheath edge forms, m

λ neutral mean free path, m

λ_{av} average neutral mean free path for mercury atoms in orifice channel, m

λ_e mean free path for fast electrons with respect to exciting or ionizing collisions, m

λ_{eo} mean free path for fast electrons with respect to exciting or ionizing collisions in hollow-cathode interior, m

σ neutral cross section of mercury atoms, 7.1×10^{-20} m^2

σ_e approximate first ionization (or excitation) cross section of mercury, 10^{-20} m^2

APPENDIX B

LANGMUIR PROBE DATA ANALYSIS

At large negative probe potentials, a saturation ion current is drawn and no electron current. Over some region of moderate probe potentials, electrons of sufficient thermal energy reach the probe in spite of the retarding field. At and beyond plasma potential, a saturation electron current is drawn, which is much greater in absolute value than the ion saturation current.

The electron temperature is obtained from the electron current in the retarding region. The value of this current is measured from a base line obtained by extending the ion saturation current line toward positive potentials.

This current is plotted on the logarithmic scale of semilogarithmic paper against the corresponding voltage. Generally, a straight line is obtained over one to two orders of magnitude. The straight line is an indication of a Maxwellian distribution of electron energies and the corresponding temperature expressed in electron volts is given by

$$V_e = \frac{\Delta V_{pr}}{2.3} \tag{B1}$$

where ΔV_{pr} is the change in probe voltage in volts over a decade of change in current.

Next, straight portions of the semilogarithmic plot over and under the knee of the curve are extended, and the coordinates of the intersection of the straight lines indicate approximately the value of the plasma potential and the electron saturation current. Because of complicated effects involving a change in the sheath dimension around the probe as the probe potential is increased, it is often somewhat ambiguous how the extension of the upper portion of the curve should be drawn. This introduces considerable uncertainty in the saturation current. The uncertainty in the plasma potential is less pronounced due to the steepness of the low portion of the curve, which is well defined.

The value of the saturation electron current together with the electron temperature yields the electron number density given in mks units as

$$n_e = 3.74 \times 10^{13} \frac{J_{pr}}{A_{pr} V_e^{1/2}} \tag{B2}$$

where A_{pr} is the active area of the probe and J_{pr} is the saturation current to the probe.

APPENDIX C

ESTIMATION OF DENSITIES FOR NEUTRAL EFFLUX

The density variation of mercury vapor in the discharge region is estimated by considering an efflux of neutral vapor from a cylindrical orifice channel 1 millimeter long and 0.2 millimeter in diameter but neglecting the slight taper of less than 3^{o} half-angle of the actual orifice used. Also, the external pressure in the bell jar (about 10^{-6} torr) is considered negligible with respect to the pressure in the tip cavity.

In the first approximation, one may consider a system in which an ideal gas of pressure p in a large container exhausts into vacuum through a small orifice of radius R and of negligible length. The arrival rate $\dot{N}$ of atoms (in mks units) at the orifice plane, hence, the flow rate through such an orifice, is

$$\dot{N} = \frac{1}{4} n\bar{v}A = \frac{1}{4} n \left(\frac{8kT}{\pi m}\right)^{1/2} A = 2.57nT^{1/2} A \tag{C1}$$

where the expression for the average thermal velocity $\bar{v}$ has been used, T is the absolute temperature, k is the Boltzmann constant, m is the mass of the mercury atom, A is the area of hole, and n is the number density of atoms behind the orifice. This relation assumes free molecular flow.

Under the actual experimental situation, one wishes to examine the effect of orifice channel length and the possible discrepancy if conditions are such that the flow is other than free molecular. An expression given by Dushman (ref. 10) relates the arrival rate at the exit hole which must equal the measured mercury flow rate J_{Hg}

$$J_{Hg} = \left(1 + \frac{3}{8}\frac{L}{R}\right)^{-1} \left(1 + 0.15 \frac{R}{\lambda_{av}}\right) N_o \tag{C2}$$

where λ_{av} is the average mean free path of mercury atoms in the channel. The first factor on the right side of equation (C2) is known as the Clausing factor and it corrects for the orifice length. The second parenthesis is an empirical correction factor which allows for the possibility that the flow is not free molecular.

The mean free path in general is related to the number density by the relation

$$\lambda = \frac{1}{\sqrt{2}\, n\sigma} \tag{C3}$$

where σ is the neutral cross section of mercury atoms, 7.1×10^{-20} square meters. The average mean free path in equation (C2) is understood to be a spatial average of its value over the length of the orifice channel. By equation (C3), this is related to the spatial average of the number density. This spatial average was taken as

$$n_{av} = \frac{1}{2}(n_o' + n_1) \tag{C4}$$

where n_o' is the atom density in the cavity behind the upstream hole, for free molecular flow, and n_1 is the atom density in the orifice channel near the downstream hole. These densities may be calculated from arrival rates by equations (C1) and (C2), letting the second correction factor in (C2) go to 1 for free molecular flow. With the two corrections factors determined, equations (C1) and (C2) yield a corrected atom density n_o inside the cavity behind the upstream hole for a given vapor temperature T and mercury flow J_{Hg}.

To obtain numerical values, one must make some reasonable estimate of the vapor temperature inside the hollow-cathode tip. External pyrometric and thermocouple measurements may differ from the actual inside temperature appreciably. The uncertainty in the density estimates, arising from lack of definite knowledge of this temperature, can be gaged by choosing two values that are believed to represent the extremes of the range of estimates of possible internal temperatures.

Table III lists the values of n_1, n_o', and n_o for the temperatures of 1300 and 5000 K. The number densities of atoms are calculated for a flow of 50 equivalent milliamperes, equal to 3.0×10^{17} atoms per second. It is clear from the table that the simple estimate of the density (and pressure) based on equation (C1) and on a temperature anywhere in the range of 1300 to 5000 K would have yielded a value within about an order of magnitude of those calculated with the corrections.

Also, the spatial variation of the pressure over the length of the orifice channel remains within the uncertainty of such an estimate. Therefore, for order-of-magnitude calculations, the assumption of uniform vapor density inside the cavity and the use of the uncorrected free-molecular-flow expression for a flat orifice is probably adequate.

To determine the density distribution downstream of the orifice requires knowing the efflux pattern, and this in turn requires a knowledge of the flow regime inside the orifice.

The Knudsen number K is defined as

$$K = \frac{\lambda}{2R} \tag{C5}$$

and the numerical values obtained for the conditions prevailing in the orifice channel based on average mean free paths range from 0.15 to 0.3 for the temperatures between 1300 and 5000 K. This means that the flow is in an intermediate regime between "slip flow" ($0.015 < K < 0.15$) and free molecular flow ($K > 5$), but much closer to the former than to the latter.

In reference 8 (p. 33) an experimental slip-flow efflux pattern from a channel of $L/R = 8$ is shown to have a near-cosine distribution. These arguments indicate that, to a fair approximation, Knudsen's equation (eq. (B10) of ref. 8) describes the neutral efflux from the hollow-cathode orifice when no discharge is drawn from the cathode.

REFERENCES

1. Breton, Claude: Hollow-Cathode Arcs: Literature Survey. Rep. CEA-BIB-88, CEA-EURATOM, Mar. 1967.

2. Kerslake, William R.; Byers, David C.; and Staggs, John F.: SERT II Experimental Thruster System. Paper No. 67-700, AIAA, Sept. 1967.

3. Rawlin, Vincent K; and Pawlik, Eugene V.: A Mercury Plasma-Bridge Neutralizer. Paper No. 67-670, AIAA, Sept. 1967.

4. Bechtel, R. T.; Csiky, G. A.; and Byers, D. C.: Performance of a 15-Centimeter Diameter, Hollow-Cathode Kaufman Thruster. Paper No. 68-88, AIAA, Jan. 1968.

5. Kemp, Robert F.; and Hall, David F.: Ion Beam Diagnostics and Neutralization. Rep. TRW-06188-6011-R000, TRW Systems Group (NASA CR-72343), Sept. 11, 1967.

6. Kiefer, L. J.; and Dunn, G. H.: Electron Impact Ionization Cross Section Data for Atoms, Atomic Ions and Diatomic Molecules. I - Experimental Data. Rep. 51, Joint Inst. Lab. Astrophysics, Univ. Colorado, Oct. 11, 1965.

7. Tonks, Lewis; and Langmuir, Irving: A General Theory of the Plasma of an Arc. Phys. Rev., vol. 34, no. 6, Sept. 15, 1929, pp. 876-922.

8. Cook, Harlan; and Richley, Edward A.: Measurements of Efflux Patterns and Flow Rates from Cylindrical Tubes in Free-Molecule and Slip Flows. NASA TN D-2480, 1964.

9. Davis, J. W.; Walch, A. P.; and Pinsley, E. A.: The Annular Hollow Cathode - Its Operation and Applications. Proceedings of Eighth Annual Electron and Laser Beam Symposium. G. I. Haddad, ed., Univ. of Michigan, 1966, pp. 217-231.

10. Dushman, Saul: Scientific Foundations of Vacuum Technique. John Wiley & Sons, Inc., 1949.

TABLE I. - COMPARISON OF CHARACTERISTIC PROPERTIES OF SPOT AND PLUME MODES

Characteristics (typical values)	Spot	Plume
Appearance	Intense spot within a few mm radius from exit hole	Luminous bluish plume-like region extending from cathode to about two-thirds of distance to anode
Neutral flow, J_{Hg}, equivalent mA	~50 and higher	~50 and lower
Discharge current, J_I, A	2.0	0.3
Electron to atom ratio, J_I/J_{Hg}	40	6
Discharge voltage, ΔV_I, V	13.5	35
Plasma potential (with respect to cathode),[a] V	11	11
Electron density (0.5 cm from cathode), n_e, electrons/m^3	10^{18}	10^{17}
Electron temperature,[a] V_e, V	0.5	1.0 to 2.3
Estimated ionization fraction, n_e/n	0.1 to 1.0	0.01 to 0.1
Tip temperature (pyrometer), K	1600	1350

[a]For region between cathode and anode.

TABLE II. - COMPARISON OF ESTIMATED ATOM DENSITIES AND MEASURED ELECTRON DENSITIES

Distance from cathode along symmetry axis, cm	Estimated atom density,[a] atoms/m^3	Measured electron density,[b] electrons/m^3	
		Spot mode	Plume mode
0.5	5×10^{18}	$>10^{18}$	$\sim10^{17}$
1.0	8×10^{17}	6×10^{17}	2×10^{16}
2.0	3×10^{17}	2×10^{17}	3×10^{15}

[a]In absence of discharge, based on 50-equivalent-mA neutral flow.
[b]Anode distance, 3 cm.

TABLE III. - COMPARISON OF NEUTRAL ATOM DENSITY ESTIMATES AND CORRESPONDING PRESSURES FOR THE INTERIOR OF THE HOLLOW CATHODE WITH A MERCURY FLOW OF 50 EQUIVALENT MILLIAMPERES

Location	Temperature, T, K			
	1300		5000	
	Density, atoms/m^3	Pressure, torr	Density, atoms/m^3	Pressure, torr
In orifice channel near downstream hole	1.1×10^{23}	14	5.4×10^{22}	28
In cavity behind upstream hole:				
Free molecular flow	5.2×10^{23}	66	2.6×10^{23}	135
Corrected flow	3.6×10^{23}	46	2.1×10^{23}	105

[a]Based on flow rate, $J_{Hg} = 3.0\times10^{17}$ atoms/sec.

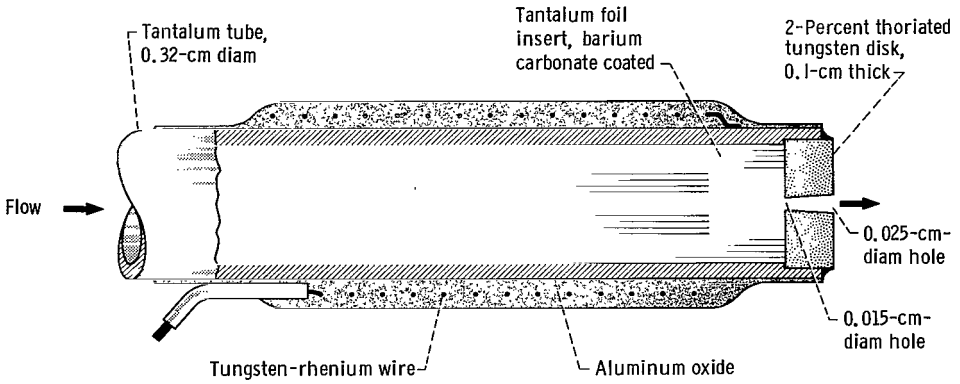

Figure 1. - Hollow-cathode tip.

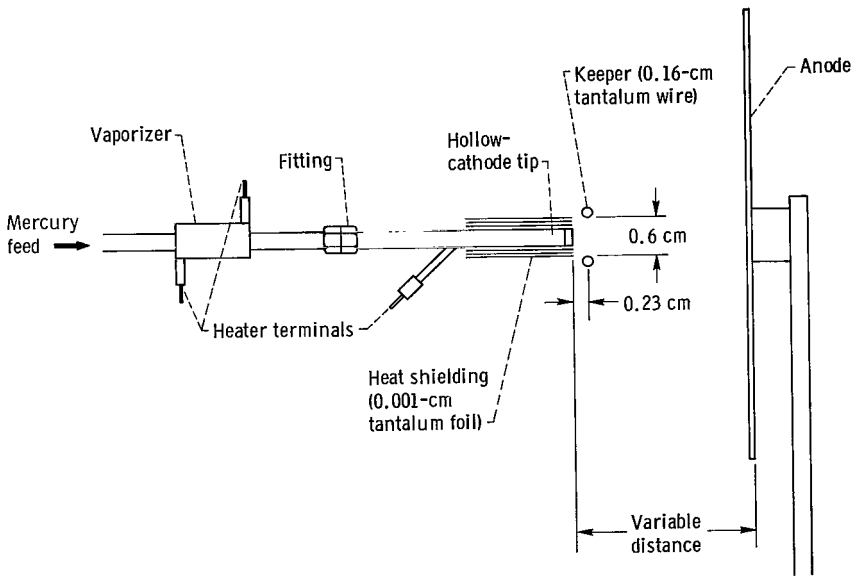

Figure 2. - Experimental arrangement of hollow-cathodes tests in bell jar.

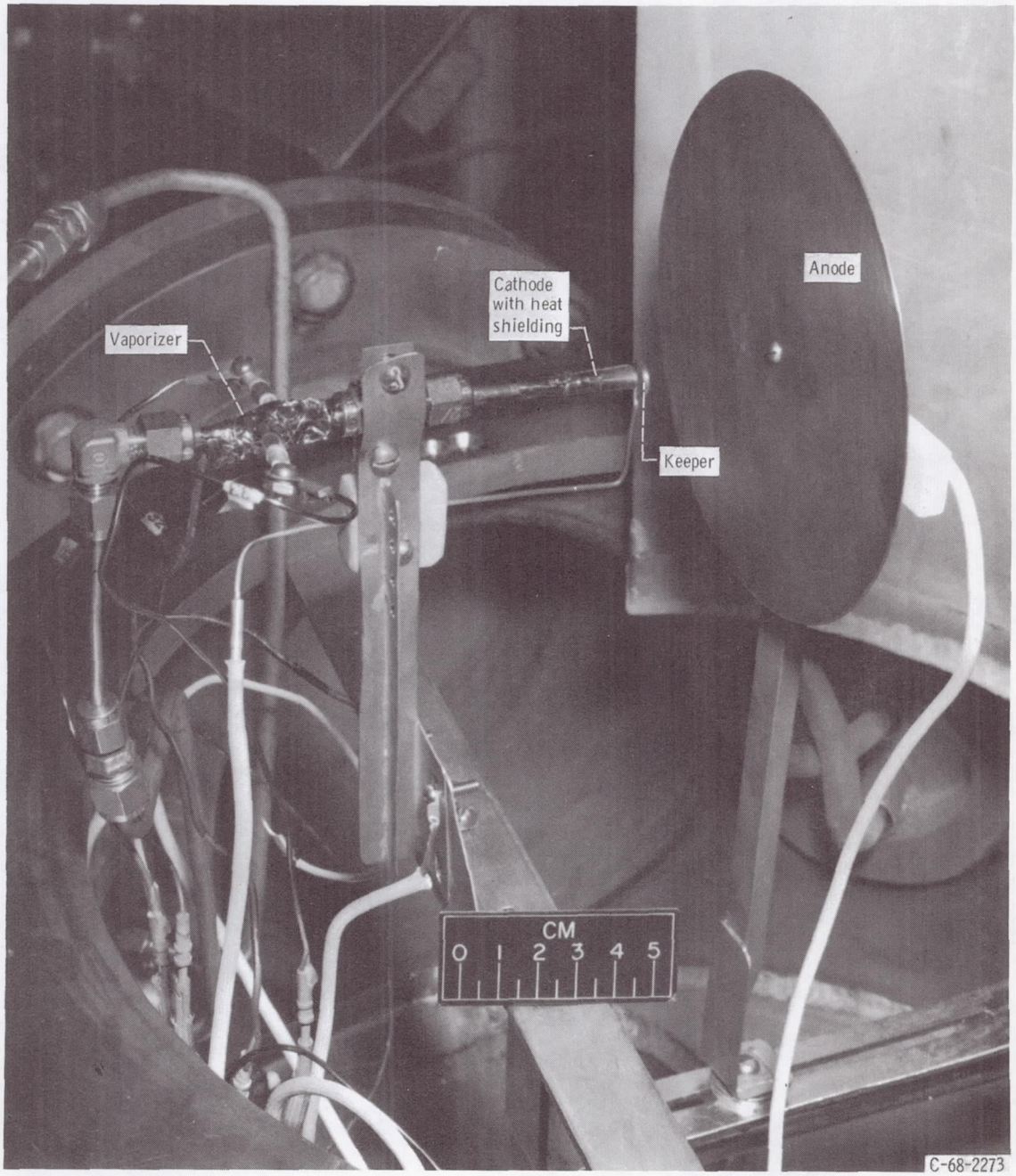

Figure 3. - Experimental arrangement in bell jar.

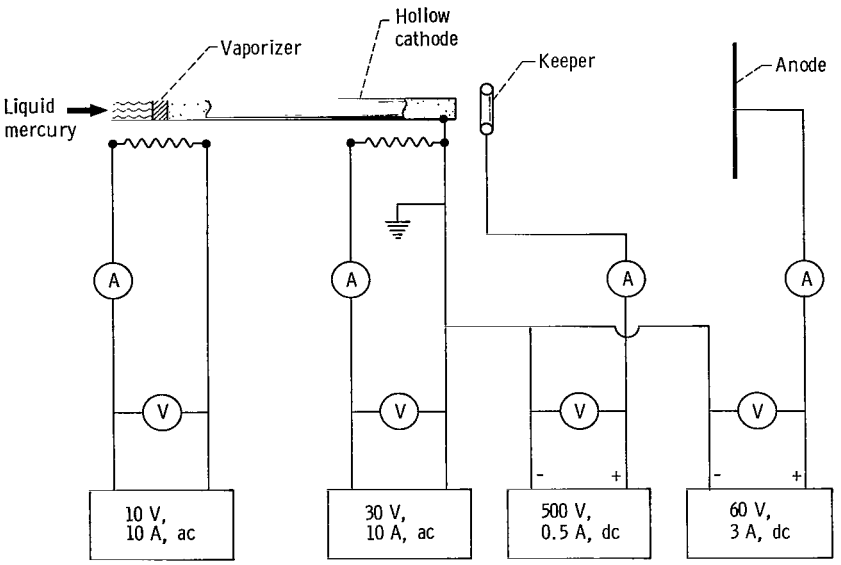

Figure 4. - Electrical circuit schematic with keeper electrode in use.

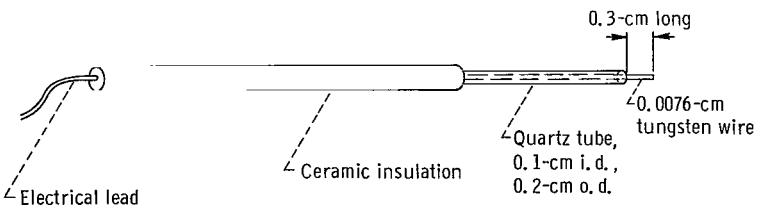

Figure 5. - Langmuir probe construction.

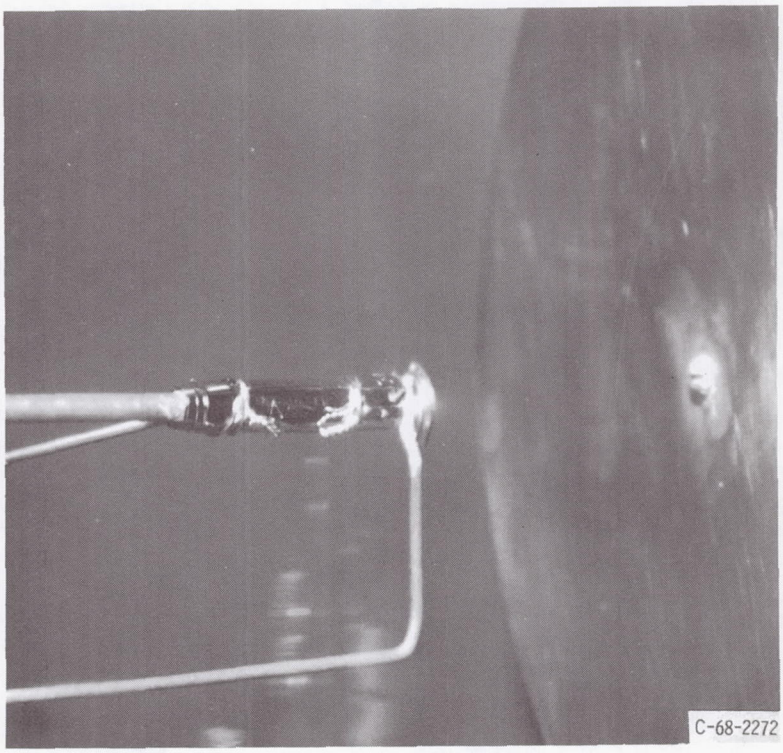

(a) Spot mode.

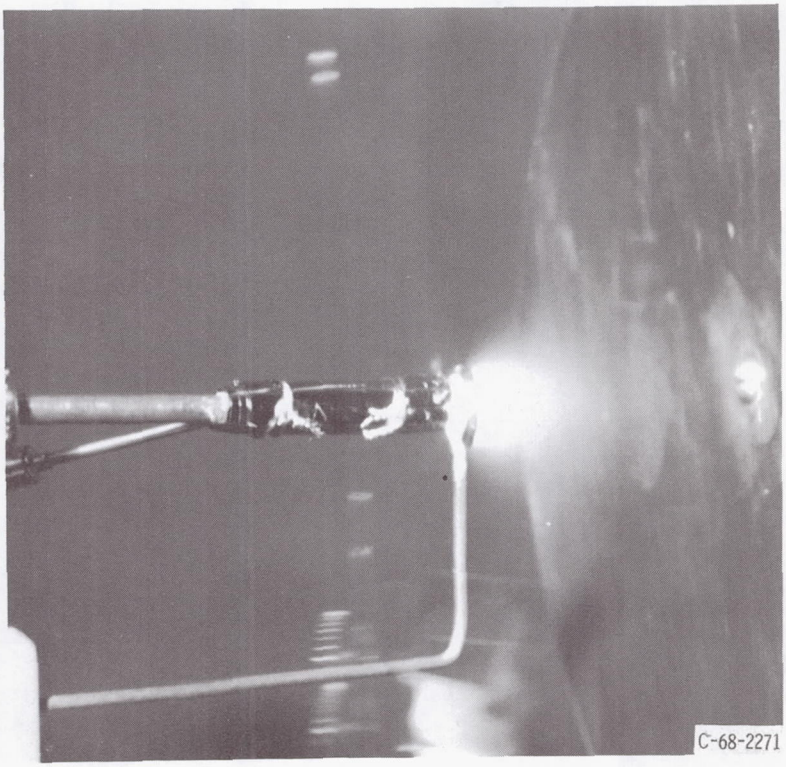

(b) Plume mode.

Figure 7. - Visual appearance of discharge in the two modes.

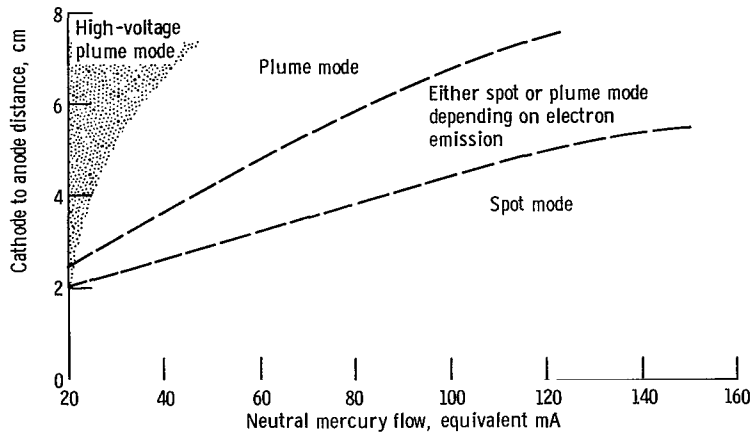

Figure 8. - Ranges of anode distance and neutral flow for various discharge modes.

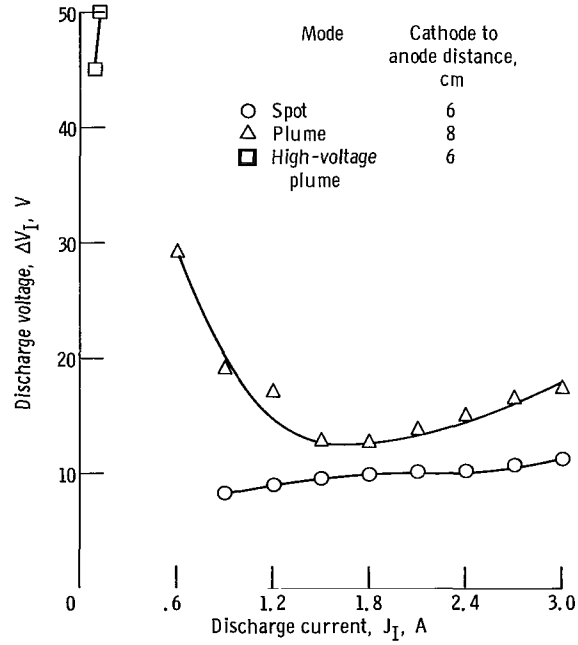

Figure 9. - Voltage-current characteristics of hollow-cathode discharge in various modes. Anode, 14-centimeter-diameter circular plate; neutral flow, 120 equivalent milliamperes.

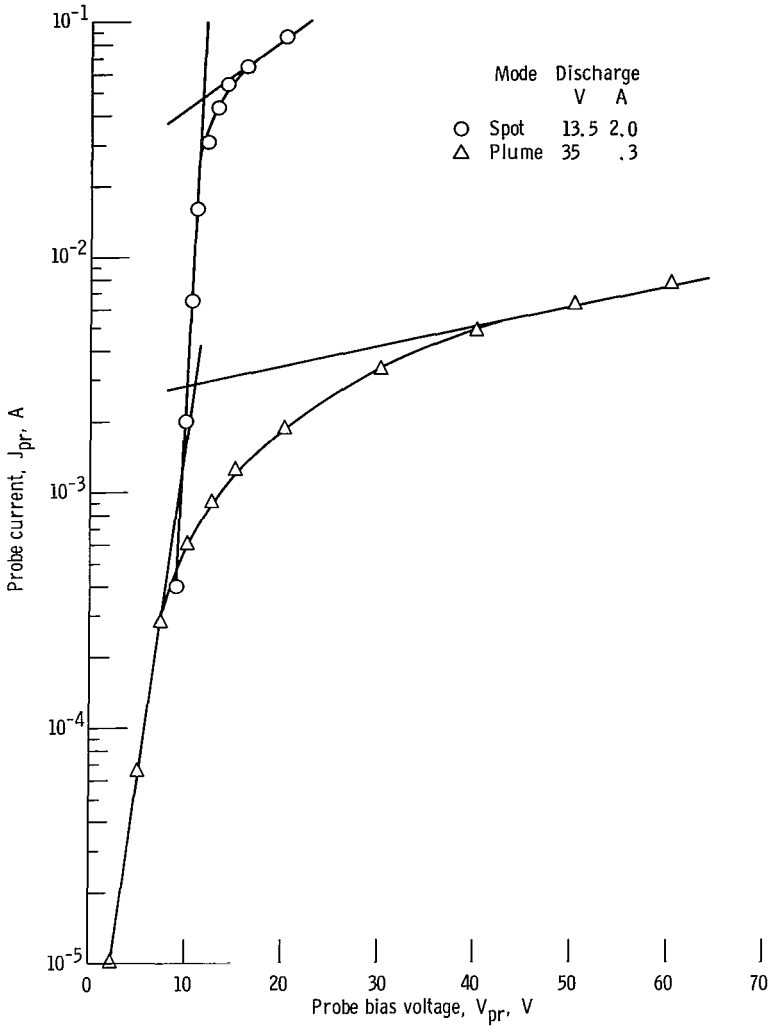

Figure 10. - Semilogarithmic plots of typical Langmuir probe traces. Position of probe, 1.0 centimeter from cathode tip on symmetry axis.

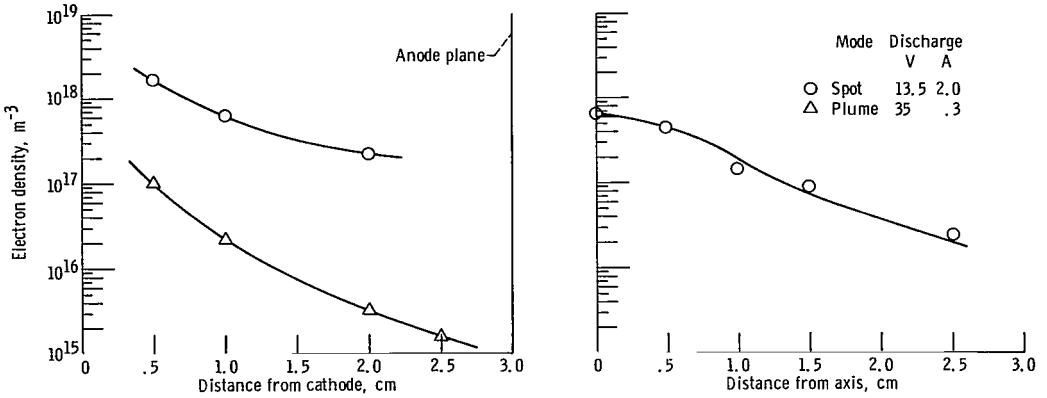

(a) Positions along symmetry axis.

(b) Radial positions in a plane 1 centimeter from cathode.

Figure 11. - Electron density distribution in hollow-cathode discharge obtained with Langmuir probe. Approximate neutral flow, 50 equivalent milliamperes.

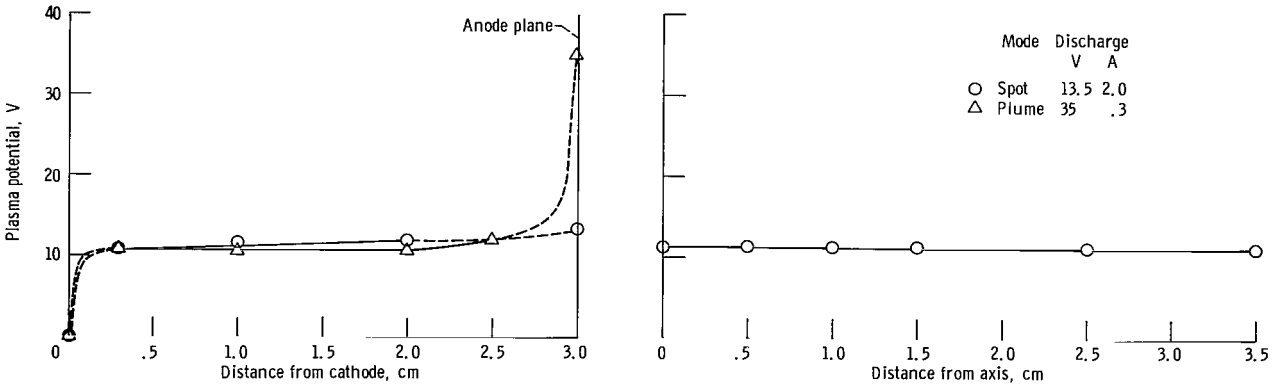

(a) Positions along symmetry axis.

(b) Radial positions in a plane 1 centimeter from cathode.

Figure 12. - Plasma potential distribution in hollow-cathode discharge obtained with Langmuir probe potential measured with respect to cathode. Approximate neutral flow, 50 equivalent milliamperes.

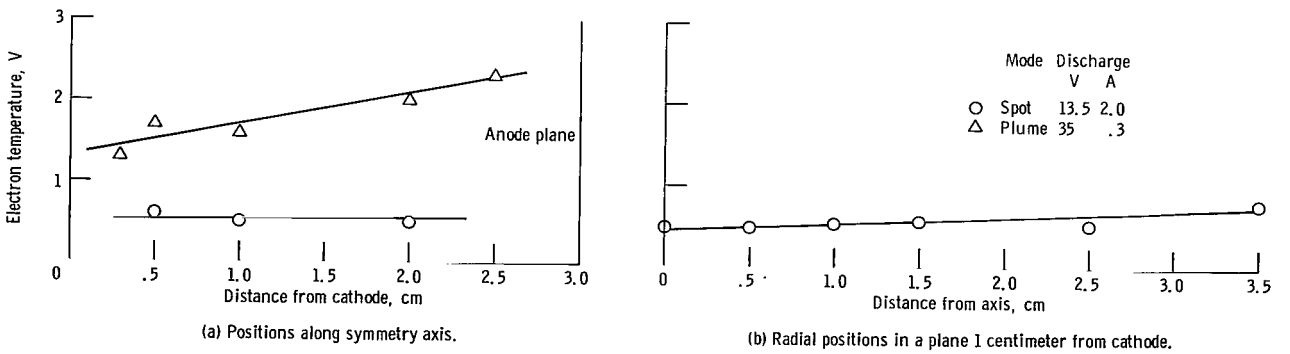

(a) Positions along symmetry axis.

(b) Radial positions in a plane 1 centimeter from cathode.

Figure 13. - Electron temperature distribution in hollow-cathode discharge obtained with Langmuir probe. Approximate neutral flow, 50 equivalent milliamperes.

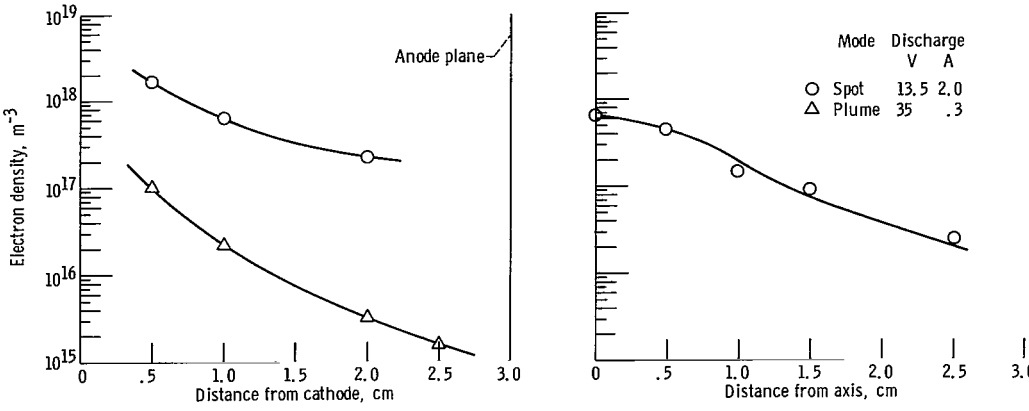

(a) Positions along symmetry axis.

(b) Radial positions in a plane 1 centimeter from cathode.

Figure 11. - Electron density distribution in hollow-cathode discharge obtained with Langmuir probe. Approximate neutral flow, 50 equivalent milliamperes.

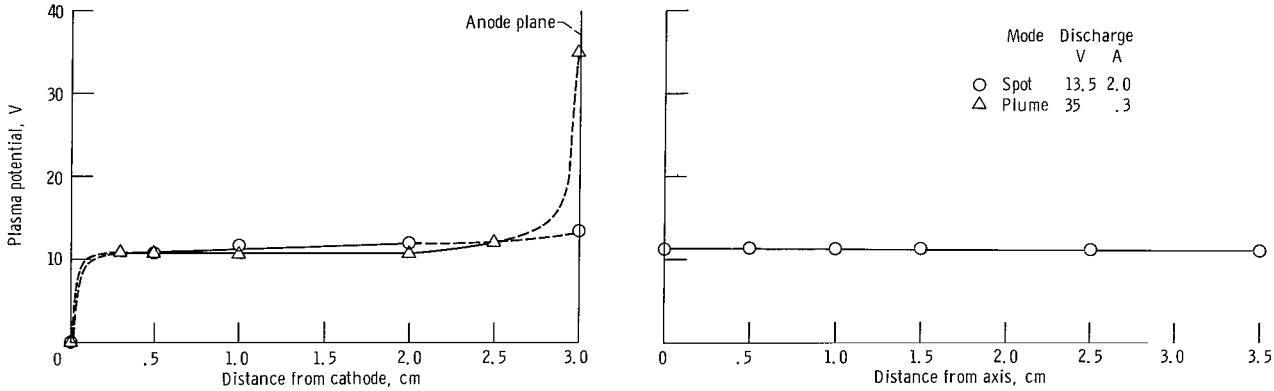

(a) Positions along symmetry axis.

(b) Radial positions in a plane 1 centimeter from cathode.

Figure 12. - Plasma potential distribution in hollow-cathode discharge obtained with Langmuir probe potential measured with respect to cathode. Approximate neutral flow, 50 equivalent milliamperes.

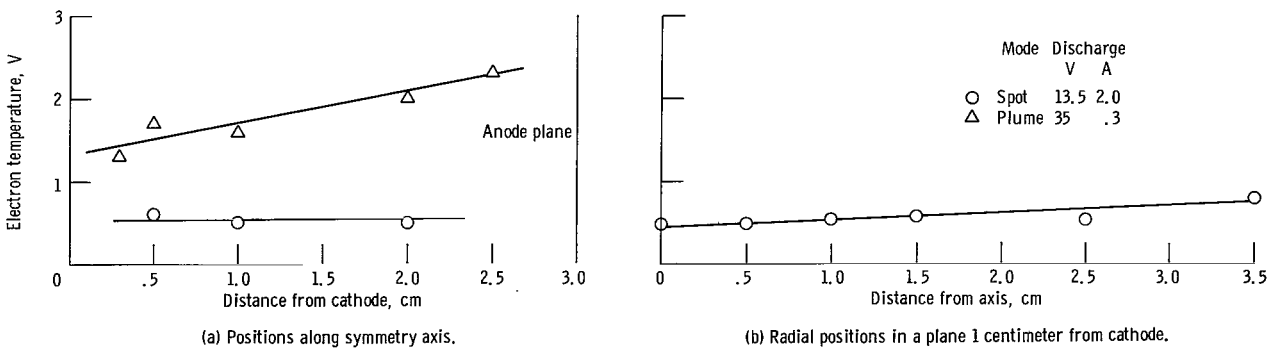

(a) Positions along symmetry axis.

(b) Radial positions in a plane 1 centimeter from cathode.

Figure 13. - Electron temperature distribution in hollow-cathode discharge obtained with Langmuir probe. Approximate neutral flow, 50 equivalent milliamperes.

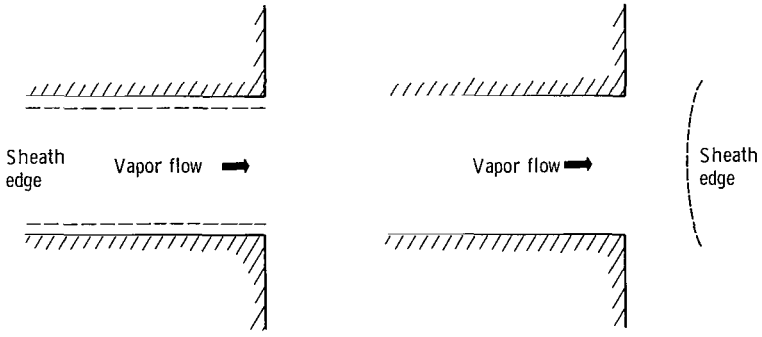

(a) Spot mode. (b) Plume mode.

Figure 14. - Illustration of hypothetical sheath-edge positions in orifice channel cross section.

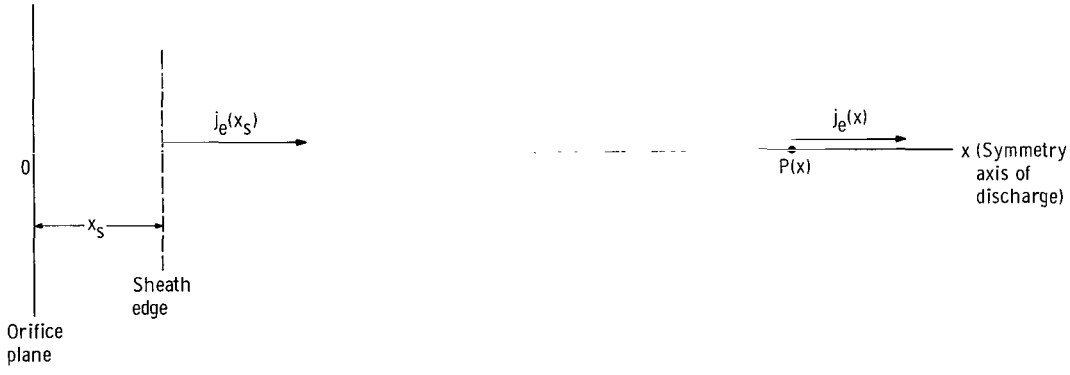

Figure 15. - One-dimensional representation of fast-electron flow density along discharge axis.

"The aeronautical and space activities of the United States shall be conducted so as to contribute . . . to the expansion of human knowledge of phenomena in the atmosphere and space. The Administration shall provide for the widest practicable and appropriate dissemination of information concerning its activities and the results thereof."

—NATIONAL AERONAUTICS AND SPACE ACT OF 1958

NASA SCIENTIFIC AND TECHNICAL PUBLICATIONS

TECHNICAL REPORTS: Scientific and technical information considered important, complete, and a lasting contribution to existing knowledge.

TECHNICAL NOTES: Information less broad in scope but nevertheless of importance as a contribution to existing knowledge.

TECHNICAL MEMORANDUMS: Information receiving limited distribution because of preliminary data, security classification, or other reasons.

CONTRACTOR REPORTS: Scientific and technical information generated under a NASA contract or grant and considered an important contribution to existing knowledge.

TECHNICAL TRANSLATIONS: Information published in a foreign language considered to merit NASA distribution in English.

SPECIAL PUBLICATIONS: Information derived from or of value to NASA activities. Publications include conference proceedings, monographs, data compilations, handbooks, sourcebooks, and special bibliographies.

TECHNOLOGY UTILIZATION PUBLICATIONS: Information on technology used by NASA that may be of particular interest in commercial and other non-aerospace applications. Publications include Tech Briefs, Technology Utilization Reports and Notes, and Technology Surveys.

Details on the availability of these publications may be obtained from:

SCIENTIFIC AND TECHNICAL INFORMATION DIVISION

NATIONAL AERONAUTICS AND SPACE ADMINISTRATION

Washington, D.C. 20546